A Spin Probe Study of Mesoporous Silica Formation via a Neutral Templating Route

Horia Caldararu,* Agneta Caragheorgheopol, and Florenta Savonea

Romanian Academy, Institute of Physical Chemistry "I. G. Murgulescu", Splaiul Independentei 2002, 77208 Bucharest, Romania

Duncan J. Macquarrie* and Bruce C. Gilbert

University of York, Department of Chemistry, Heslington, York, YO10 5DD, U.K.

Received: April 18, 2002; In Final Form: December 3, 2002

The structure of dodecylamine (DDA) aggregates acting as templates in the synthesis of mesoporous silica (in the DDA/water/ethanol/tetraethoxysilane (TEOS) system) has been studied via the EPR spectra of a variety of spin probes and of a spin-labeled silica precursor. Two recipes have been examined: one, starting from a water-rich DDA solution, $\mathbf{A_0}$, reported to produce a silica with framework mesopores and textural pores comparable in volume, and another, starting from an ethanol-rich solution, $\mathbf{B_0}$ which yields a solid having practically only framework pores. For both compositions the relative positions of the spin probes in the aggregates have been determined, the local polarities expressed in terms of the Kosower scale and their motions examined. The aggregates formed have been characterized as emulsion droplets for $\mathbf{A_0}$ and micelles with radii <25 Å for $\mathbf{B_0}$. After reaction of $\mathbf{A_0}$ and $\mathbf{B_0}$ with TEOS, all probes showed significantly hindered motion in the wet precipitates. In the solid **B**, precipitated from the ethanol-rich solvent, the spin probes 5- and 7-doxyl stearic acid (5- and 7-DSA) are strongly immobilized, while other probes maintain quasi-isotropic motion but with very large rotational correlation times. This pattern is characteristic of micelles with hindered tumbling and/or lateral diffusion and is assigned to those aggregates (in interaction with the silica component) on which the framework mesopores are formed. In solid **A**, precipitated from $\mathbf{A_0}$, 5- and 7-DSA spin probes maintain the spectra with anisotropic features, characterized by an order degree, found in the starting emulsion, but with evidence of tighter packing, while other probes have their rotation retarded. These aggregates have a low curvature interface, characteristic of emulsion droplets and are assumed to be at the origin of the large textural pores, which characterize this solid. Adsorption of probes after synthesis rather than before precipitation supports these assignments. We have also found that the surfactant−silica interaction is critically dependent on solvent. The strong immobilization of the probes in the interface region, observed during drying at low temperatures, is a reversible process, since under these conditions the silica network cross-linking is only incipient; ^{29}Si NMR data show that cross-linking becomes important only above 90 °C.

Introduction

The discovery of the M41S class of mesoporous silicas by Beck and co-workers[1] in 1992 opened the way forward for fundamental research on their synthesis and applications, as well as on the phenomena which occur when mixtures of the colloidal surfactant solution and the inorganic precursor lead to the templated synthesis of the mesoporous silicas.[2]

Synthesis of organically modified silicas has been attempted both as postsynthesis modification of preformed MCMs and as a one-step procedure, when the organosilane is copolymerized with the silica precursor in the presence of the templating agent.[3−8] This last approach implies a mild treatment of the silica for removal of the template and the use of a neutral surfactant as template. The synthesis described by Pinnavaia and co-workers,[9,10] using dodecylamine (DDA) as the templating surfactant in ethanol/water mixtures and tetraethoxysilane (TEOS) as the silica precursor, was adopted by one of us in the synthesis of organically modified silicas.[3] This pathway offers many advantages over the original route,[1] such as very mild processing (formation and extraction) conditions, the ability to incorporate organics successfully, and the possibility of recovering template after reaction. Despite the potential utility of these materials as catalysts, little work has been published which gives insight into their formation.

Pinnavaia and co-workers[9] have investigated the role of the solvent polarity (ethanol/water ratio) on the pore structure of the resulting silica. In water-rich compositions, mesostructures result with a wormholelike framework structure with complementary textural pore volumes comparable in magnitude to the framework−pore volume. In ethanol-rich mixtures the same wormhole framework is produced, but the textural porosity is less than 20% (usually 5%) of the framework pore volume. Transmission electron microscopy (TEM) images indicate quite clearly that, regardless of the solvent system used, regular framework pores originate from the space originally occupied by the uniform surfactant assemblies. The study[9] shows that the catalytic activity of these mesoporous silicas for a sterically demanding condensed-phase reaction is enhanced by the textural mesoporosity, required for the transport of the reagents to the framework mesopores. However, while the role of the solvent polarity on the pore structure has been elucidated,[9] no details on their formation at molecular level were provided by these methods.

The aim of this study—as a first step in the study of the synthesis of functionalized silicas—was to investigate, at the

* Corresponding author.

10.1021/jp021004o CCC: $25.00
Published on Web 06/04/2003

molecular level, the self-assembled aggregates formed by dodecylamine (DDA) in two ethanol/water mixtures (in the water-rich and ethanol-rich regions, respectively) and to follow the changes of these aggregates by interaction with the inorganic precursor in the templated synthesis of mesoporous silica. For this purpose, the use of EPR of spin probes is a particularly suitable method, since, as has been widely demonstrated in the field of colloidal systems, the paramagnetic species (stable organic radicals) used as probes dissolve in different parts of the microheterogeneous system and provide information about the local polarity, structure, and dynamics.[11,12] The technique has been used by Bakker et al.[13,14] to obtain information about the structure of surfactant aggregates adsorbed on nonporous silica surfaces. Goldfarb et al.[15,16] and Ottaviani et al.,[17,18] have used the same technique to follow the electrostatic charge matching assembly pathway in the MCM-41 synthesis.

Our approach to the study of the neutral pathway consists of using a number of spin probes (structures **1**−**3**) with different

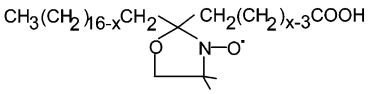

(1) *x*-DSA

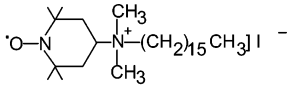

(2) CAT 16

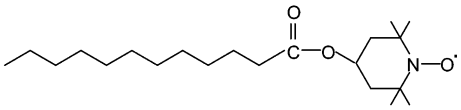

(3) C_{12}-NO

properties (cationic, neutral and anionic) and with the label at different distances from the anchor (the series of *x*-DSA) in order to characterize the nature of the starting colloidal system (DDA in different ethanol/water mixtures). A spin-labeled silica precursor (structure **4**), expected to mimic the behavior of the

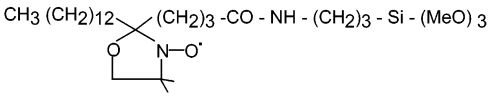

(4) doxyl -TMOS

inorganic component, has been used too. The spectral changes have then been followed after addition of TEOS in the as-synthesized wet precipitates, as well as after their mild thermal treatment. Finally the spectra have been compared to those which result from adsorption of the spin probes after synthesis.

Experimental Part

Materials. Dodecylamine (Aldrich, 98%), absolute ethanol (Fisher), tetraethoxysilane (Avocado, 98%), 3-aminopropyltrimethoxysilane, *N*,*N*′-dicyclohexylcarbodiimide (DDC), 3-carboxy-Proxyl (Sigma), and distilled water were used throughout.

The spin probes of the *x*-doxyl stearic acid series, (*x*-DSA) ($x = 5$, 7, 10, and 16) were from SIGMA, CAT 16 was from Molecular Probes and TEMPO-laurate (C_{12}−NO) was prepared as described.[19]

The spin-labeled silica precursor (doxyl-TMOS), *N*-propyltrimethoxysilane-5-doxylstearamide has been synthesized as follows: 10 mg of 3-aminopropyltrimethoxysilane, 10 mg of 5-DSA and 20 mg of DDC were mixed in anhydrous methylene chloride and left for 5 days at room temperature to complete the reaction. ESI-MS measurements show no peak corresponding to 5-DSA and indicate the presence of the labeled compound: $C_{28}H_{59}N_2O_7Si$, 546 (M^+). The EPR spectrum in tetrahydrofuran has an a_N value of 16.45 G.

Sample Preparation. *DDA/Ethanol/Water Solutions.* A number of compositions with different ethanol/water weight ratios (80/20, 70/30, 60/40, 50/50, 40/60, 30/70, 20/80, and 10/90) were prepared. DDA was dissolved in them below the solubility limit at 20 °C. The lower the alcohol content, the lower the DDA solubility.

Two compositions were selected as starting solutions for the silica preparation:

$$\mathbf{A_0} = \text{DDA/EtOH/water} = 0.255/0.8/4.0\ \text{(g/g/g)}$$

$$\mathbf{B_0} = \text{DDA/EtOH/water} = 0.255/1.84/2.65\ \text{(g/g/g)}$$

To the solutions $\mathbf{A_0}$ and $\mathbf{B_0}$, 0.55 g and, respectively, 1.04 g of TEOS have been added to yield the corresponding reaction mixtures. The spin probes and spin-labeled derivative were added to aliquots of the starting solutions in low concentration (10^{-4} M). The precipitation started immediately after mixing. After the reaction completion (18 h), or earlier in some cases (where indicated), the precipitate (**A** and, respectively, **B**) was filtered and well washed on the filter with warm ethanol/water solutions in the proportion used in the synthesis. In all cases the washing was continued until no probe was detected by EPR in the filtrate. Then, the solid was mixed again with water and centrifuged, after which both the wet solid and the liquid were examined separately by EPR. The solids were then dried at different temperatures and the evolution of the spectra was followed. In a few cases the presence of the spin probes in the solid was checked after complete surfactant removal by extraction with ethanol. The materials were finally extracted with hot ethanol and the porosity determined.

The adsorption of the spin probes was followed on the final mesoporous materials, $\mathbf{A_f}$ and $\mathbf{B_f}$, after removal of the surfactant. Small quantities of the two solids were immersed in the starting solutions, with spin probes included (10^{-4} M) and left overnight without stirring or, alternatively, 2 days with stirring. Then, the solids were filtered and washed as described above. The EPR spectra of the adsorbed spin probes were measured in the wet solids.

EPR Spectra. The EPR spectra were recorded on a RE1X JEOL spectrometer with 100 kHz field modulation using X-band frequency. The ^{14}N isotropic hyperfine splitting, a_N, the polarity-sensitive parameter,[20] was measured directly from the three sharp line spectra. An approximate value of the rotational correlation time, τ_C, was calculated according to the formula[21]

$$\tau_C = (6.51 \times 10^{-10})\Delta H(0)\{[h(0)/h(-1)]^{1/2} + [h(0)/h(1)]^{1/2} - 2\}\ \text{s}$$

where $\Delta H(0)$ is the line width (in Gauss) of the central line, and $h(-1)$, $h(0)$, and $h(1)$ are the peak heights of the $M = -1$, 0, and +1 derivative lines, respectively. τ_C is connected to the local viscosity, η, by the Debye−Stokes−Einstein equation, $\tau_C = 4\pi\eta R^3/3kT$, where R is the hydrodynamic radius of the tumbling entity. The τ_C values obtained were used to follow, in a qualitative manner, significant changes in the microenvironment of the probes. For spectra of the *x*-DSA probes the order parameter, S, is calculated from the observed spectral parameters $A_{||}$ and $A_\perp$ by the formula:[22] $S = (A_{||} - A_\perp)/[A_{zz} -$

$(A_{xx} + A_{yy})/2]$, where A_{zz}, A_{xx}, and A_{yy} are the principal elements of the $\boldsymbol{A}$ tensor in absence of molecular motion and $A_{||}$ and $A_{\perp}$ are derived from experimental spectra. The order parameters S, corrected for polarity differences,[22] were calculated using the following parameters reported for doxyl probes:[23] $A_{zz} = 33.5$ G, $A_{xx} = 6.3$ G, and $A_{yy} = 5.8$ G.

Polarity Determinations. The ^{14}N isotropic hyperfine splitting, a_N, is the parameter expected to report on the local polarity in different regions of the microheterogeneous system. To compare data from different probes and to relate the a_N values to a general polarity scale, use has been made of earlier calibration of the a_N values of the spin probes, measured in a series of poly(ethylene oxide/water mixtures with different water to ethylene oxide (EO) unit molar ratios, $w = [H_2O]/[EO]$, to whom specific values, Z_K, on the Kosower polarity scale[24] have been assigned by UV−vis measurements.[25,26]

NMR Measurements. ^{29}Si NMR measurements were carried out on a Bruker Avance 400 NMR using a 4 mm rotor operating at 12 kHz rotation speed, under high-power decoupled MAS conditions (^{29}Si at 79.48 MHz). Peaks are referenced to Q8 M8 at 12.6 ppm.

Porosimetry measurements were carried out on a Micromeritics ASAP2010 instrument using dinitrogen as adsorbate. Framework pore volume (V_f) was calculated as the volume adsorbed at the top of the first inflection point (ca. $P/P_o = 0.5$ for both samples) and textural pore volume (V_t) as the volume adsorbed above this pressure.

After complete extraction of template from the precipitates, the extracted material $\mathbf{A_f}$ was found to have a framework pore volume $V_f = 0.52$ cm^3 g^{-1} and a textural pore volume $V_t = 0.43$ cm^3 g^{-1}. The surface area was 687 m^2 g^{-1}, and the average pore diameter of the framework pores was 3.0 nm, while the extracted material $\mathbf{B_f}$ was found to have a framework pore volume $V_f = 1.00$ cm^3 g^{-1} and a textural pore volume $V_t = 0.12$ cm^3 g^{-1}. The surface area was 1087 m^2 g^{-1}, and the average pore diameter of the framework pores was 2.6 nm. These values are entirely consistent with materials described in the literature, prepared in the absence of spin probes.[10] The consistency of the porosity characteristics of samples prepared by the literature method and those prepared by the route involving prolonged washing with water prior to removal of template indicates that the materials are not changed by this washing step and that no changes to the porosity of the materials are induced by the washing process.

Results and Discussion

(1) The DDA/Ethanol/Water Solutions. A preliminary inquiry concerned the phase behavior of DDA solutions in ethanol/water mixtures of different compositions. Samples with ethanol/water ≤ 20/80 were observed to be biphasic even for DDA concentrations as low as 1%, whereas for higher ethanol content monophasic, optically isotropic solutions were obtained. EPR parameters of the 5-DSA spin probe were measured for most samples. For the biphasic samples the spectra are observed to have anisotropic features (e.g., Figure 1a, left), typical of ordered surfactant aggregates, such as lamellar liquid-crystalline layers or other low-curvature interfaces,[22] which in our case are expected to be the interfaces of emulsion droplets. EPR measurements show that this specific spectral pattern belongs to the upper layer of the biphasic samples, with no signal in the lower phase. For these systems, an order parameter can be calculated. In contrast, the EPR spectra of 5-DSA in the monophasic samples (e.g., Figure 1a, right) consist of sharp three-line spectra, reflecting isotropic motion; these are typical

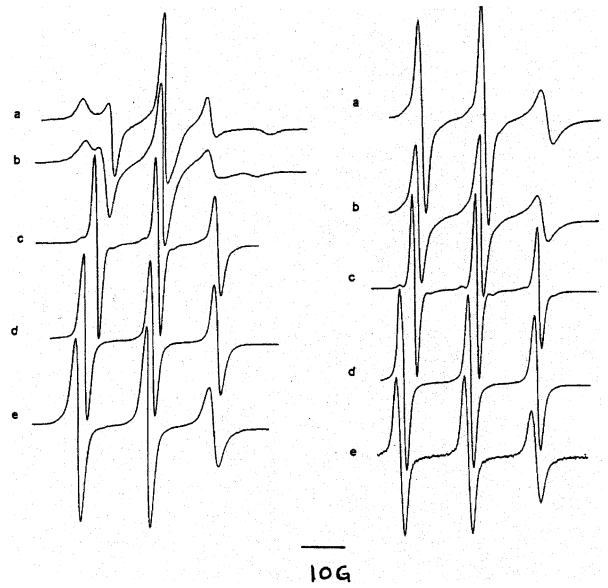

Figure 1. EPR spectra of (a) 5-DSA, (b) 7-DSA, (c) 16-DSA, (d) $C_{12}NO$, and (e) CAT 16 in the starting solutions $\mathbf{A_0}$ (left) and $\mathbf{B_0}$ (right).

of micellar aggregates with radius $R < 25-30$ Å.[27,28] The indicated size of the micelles represents the higher limit at which micellar tumbling and/or lateral diffusion of the probes around the curved surface are rapid enough to average out the anisotropic features of the "ordered" spectra. The observed change in appearance of the spectra, with the lines becoming more asymmetric as the ethanol proportion decreases, points to the gradual increase of the aggregate sizes.

Two DDA/ethanol/water compositions were selected for synthesis. One, $\mathbf{A_0}$, is in the water-rich region and is an emulsion, the other, $\mathbf{B_0}$, is from the ethanol-rich, micellar region. For an improved characterization of the surfactant aggregates in these solutions, a number of different spin probes, besides 5-DSA were used. All the spin probes used were found to be associated with the surfactant aggregates (i.e., with restricted motion, as compared to the solvent). The EPR data specific for each type of spectrum are recorded in Tables 1 and 2.

(i) Water-Rich Starting Solution, $\boldsymbol{A_0}$. Examination, first of the a_N values for the probes, when compared with the values of the same probes in a series of calibration mixtures with increasing polarity[25,26] (see Experimental Section), yields Kosower's Z_K values[24] for the sites of the different spin probes. On this basis, we find the following ordering of the position of the nitroxide moiety of the probes, from the interface toward the core (i.e. in the order of decreasing local polarity): CAT 16 > C_{12}−NO > 5-DSA > 7-DSA ≈ 16-DSA. The polarity (Z_K value) at the CAT 16 site, the closest probe to the interface, is similar to a 3% water in ethanol solution, those for the other probes being below the ethanol value.

Second, regarding the dynamics of the probes, 5-DSA presents a spectrum reflecting anisotropic rotation, rapid only around the long molecular axis (Figure 1a, left), characteristic for the probe being aligned in a tightly packed surfactant aggregate (this kind of spectrum is referred to as "with order"). The order degree, S, is calculated as 0.43. 7-DSA presents a spectrum similar to 5-DSA, but with a lower value of the order parameter (Table 1, Figure 1b, left). As expected, the mobility of the doxyl probes increases with the distance from the headgroup, which is anchored at the interface through the doxyl COO^- group. Thus, the 10-DSA spectrum has no measurable

TABLE 1: EPR Parameters of the Spin Probe Spectra in the Samples Derived from the Water-Rich Composition A_0[a]

probe	a_N (G)	τ_C (10^{10}s)	Z_K	$2A_{zz}$ (G)	$A_{\|}$ (G)	$A_\perp$ (G)	S
The Surfactant Solution $\mathbf{A_0}$							
5-DSA	14.7[b]		73.3		22.4	10.9	0.43
7-DSA	14.5[b]		< 71.6		20.6	11.4	0.35
10-DSA	~14.7	~18.1					
16-DSA	14.5	3.0	< 71.6				
C_{12}−NO	15.9	1.6	74.4				
CAT 16	16.2	7.5	80.4				
$\mathbf{A} = \mathbf{A_0}$ + TEOS, Precipitate, Filtered, Washed, Moist							
5-DSA	14.7[b]		73.3		23.8	10.1	0.52
7-DSA	14.5[b]		71.6		20.7	11.2	0.37
16-DSA	14.5	10.0	<71.6				
C_{12}−NO	15.8	7.7	72.3				
CAT 16[c]	~16.2			68.7			
A, Dried 2 h at 80 °C							
5-DSA				~66.0			
7-DSA				67.1			
16-DSA	~13.8						
C_{12}−NO[c]	15.9			67.8			
CAT 16				67.9			
A, Dried 2 h at 80 °C and 2 h at 110 °C							
5-DSA				68.7			
7-DSA				69.1			
16-DSA[c]	~13.8			66.4			
C_{12}−NO				69.8			
CAT 16				67.5			

[a] Z_K is the Kosower parameter associated with the a_N value. [b] Calculated with the formula: $a_N = {}^1/_3(A_{\|} + 2A_\perp)$. [c] Overlapping of spectra from an immobilized and a mobile species.

TABLE 2: EPR Parameters of the Spin Probe Spectra in the Samples Derived from the Ethanol-Rich Composition B_0

probe	a_N (G)	τ_C (10^{10}s)	Z_K	$2A_{zz}$ (G)
The Surfactant Solution $\mathbf{B_0}$				
5-DSA	15.0	11.1	77.7	
7-DSA	14.9	10.3	76.5	
10-DSA	*b*			
16-DSA	14.9	1.9	76.5	
C_{12}−NO	16.2	2.7	79.9	
CAT 16	16.3	3.1	83.0	
$\mathbf{B} = \mathbf{B_0}$ + TEOS, Precipitate, Filtered, Washed, Moist				
5-DSA				61.6
5-DSA[c]				62.9
7-DSA				59.2
10-DSA				58.0
16-DSA	~14.1	~26		
16-DSA[c]	~14.1	~26		
C_{12}−NO	16.2	19.2	79.9	
CAT 16				67.9
B, Dried 1 h at 50 °C				
5-DSA				68.6
7-DSA[d]	*e*		58.9	
10-DSA				58.7
16-DSA	14.4	18.0		
C_{12}−NO	16.2	19.2	79.9	
CAT 16				67.3
B, Dried 1 h at 50 °C and 2 h at 80 °C				
5-DSA				68.5
7-DSA				68.0
10-DSA				67.1
16-DSA[d]	*e*		69.2	
C_{12}−NO[d]	*e*		68.7	

[a] Z_K is the Kosower parameter associated with the a_N value. [b] Two species. [c] After 1 h of reaction. [d] Overlapping of spectra from an immobilized and a mobile species. [e] Mobile species.

order, while 16-DSA has an isotropic rotation (Figure 1c, left). C_{12}−NO and CAT 16 present typical micellar-type spectra too, with reduced tumbling rate (Figure 1d,e, left).

The two independent spectral characteristics are consistent and point to the same interpretation: the anisotropy of 5-DSA rotation is typical of aggregates with low curvature interfaces (absence of averaging by lateral diffusion or tumbling), while the relatively low polarity values (as compared to sample $\mathbf{B_0}$, see below) indicate a low degree of solvation, resulting in a low area per polar head, which in turn leads to low curvature interfaces. This description is consistent with large aggregates (low curvature of the interface), such as emulsion droplets, present in this case.

(ii) Ethanol-rich starting solution, B_0. The results obtained for this system are quite different from those described above. First, though the same order of a_N values as for $\mathbf{A_0}$ was obtained, the local polarities were systematically higher than those for $\mathbf{A_0}$. Thus, CAT 16 reports a polarity equivalent to that in a 11.4% water in ethanol mixture, while C_{12}−NO senses the polarity of a 1.2% water in ethanol solution These values testify about preferential solvation of the water insoluble surfactant (DDA), with ethanol. Next, 5- and 7-DSA present quasi-isotropic spectra (Figure 1a,b, right) where no order degree of surfactant chains can be defined; 16-DSA (Figure 1c, right) and CAT 16 (Figure 1e, right) have lower rotational correlation times in these micelles, as compared to the ones in aggregates in solution $\mathbf{A_0}$. In this case, the anisotropic spectral features of 5- and 7-DSA are averaged by lateral diffusion and/or micellar tumbling at a rate comparable with the EPR time scale (10^{-7}−10^{-8} s).[27,28] This implies an aggregate radius smaller than 25−30 Å.[27,28]

We conclude that in samples $\mathbf{B_0}$, in contrast to $\mathbf{A_0}$, the effect of increased ethanol concentration, with ethanol acting as a cosurfactant, leads to higher area per polar head, higher curvature of the aggregate surface, i.e., smaller micellar radius. The higher solvation degree is also reflected in the higher polarity values.

(2) DDA/EtOH/Water/TEOS Reaction Mixtures. After addition of TEOS to the starting solutions, the precipitation started immediately. After the mixtures were stirred for 18 h at room temperature, the suspensions were filtered, the solid precipitates were washed and their EPR spectra were measured, while moist. The spectral parameters obtained (a_N and τ_C for isotropic spectra, $A_{\|}$, $A_\perp$, and S for "ordered" spectra, $2A_{zz}$ for "immobilized" spectra) are collected in Tables 1 and 2. In some cases (see Table 2), when the reaction was stopped after 1 h, the same results were observed as after 18 h of reaction.

In the case of solid **A** (from the water-rich emulsion), the 5- and 7-DSA probes retain the ordered spectra they had in the initial solution, but with an increased order parameter (Figure 2a−c, left), while 16-DSA has a 3-fold higher rotational correlation time. For C_{12}−NO probe the mobility is even more decreased (by a factor of 5) (Figure 2d, left), while CAT 16 was found to be distributed between two types of sites: ones showing an isotropic spectrum, but with reduced mobility, and others on which it was strongly immobilized (Figure 2e, left). Thus, the surfactant aggregates appear to be influenced by the inorganic framework in the moist precipitate, the interaction leading to tighter surfactant packing.

The same trend, but with much more drastic changes was found for the solid **B** (from the ethanol-rich micellar solution) (Figure 2a−e, right). In this case all *x*-DSA probes, except 16-DSA, show immobilized type spectra. A certain decrease of the immobilization degree can be observed in the series of 5-, 7-, and 10-DSA probes; 16-DSA still shows a three-line spectrum, but close to a slow motional spectrum, with large rotational correlation time. Not only is the micellar tumbling "frozen" but also the axial rotation of the doxyl probes in the

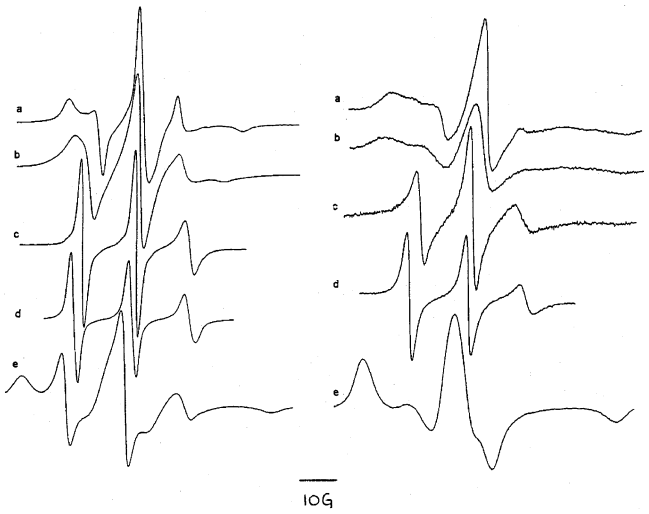

Figure 2. EPR spectra of (a) 5-DSA, (b) 7-DSA, (c) 16-DSA, (d) $C_{12}NO$, and (e) CAT 16 in the wet precipitates **A** (left) and **B** (right).

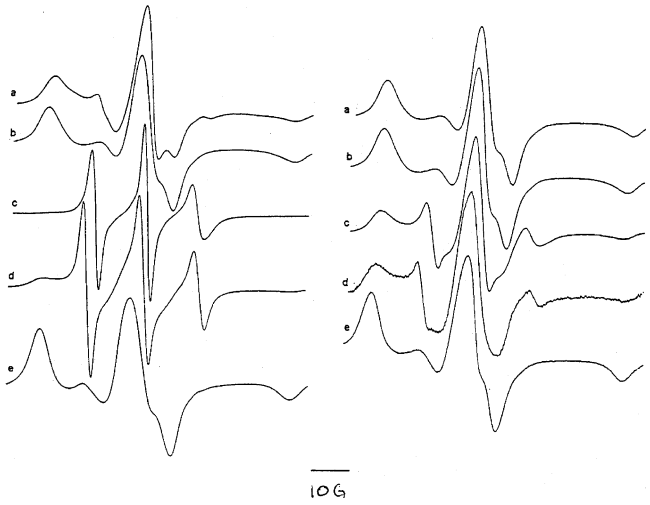

Figure 3. EPR spectra of (a) 5-DSA, (b) 7-DSA, (c) 16-DSA, (d) $C_{12}NO$, and (e) CAT 16 in the precipitates **A** (left) and **B** (right), dried 2 h at 80 °C.

micelles is blocked by the interaction of the polar head with the silica entities. $C_{12}-NO$ shows a three-line spectrum, with very large rotational correlation time. The strongly hindered motion of this probe is considered especially relevant for the surfactant, because of their close structural resemblance; it indicates a much more compact packing of the surfactant chains ($\tau_C = 19.2 \times 10^{-10}$ s) as compared to aggregates in **A** ($\tau_C = 7.7 \times 10^{-10}$ s). CAT 16 shows only the strongly immobilized spectrum. While the immobilization of CAT 16 is expected on the basis of electrostatic interaction with the anionic Si $-O^-$ sites,[15,17] the reason for doxyl probes immobilization is less obvious. The different degree of immobilization of the doxyl probes in samples **A** and **B** reflects the different strength of the interaction at the interface: thus, in the textural pores 5- and 7-DSA probes maintain rapid axial rotation, while in the framework pores the same probes appear immobilized. The difference seems to originate in the low degree of solvation of the large aggregates, leading to a weak bonding to the silica in the textural pores, while the opposite is true for the small aggregates in framework pores. The strong interaction with the silica in the last case possibly includes special effects, such as solvation by $Si-O-CH_2-CH_3$ unhydrolyzed groups (reported to occur in the final product at a density of 1.5 ethoxy groups per 10 silicon atoms[8]), by interdigitation.

When the reaction was stopped after 1 h and the solids filtered and examined, the spectra of 5-DSA and 16-DSA did not differ significantly from the final ones (Table 2).

Complete removal of the surfactant from the as-synthesized solid **B,** in samples with spin probes included showed that CAT 16 remained attached to the solid, with solidlike immobilized spectra, while $C_{12}-NO$ was completely removed with the surfactant during extraction with ethanol. Under the same conditions, 5-DSA showed an extremely broad, weak spectrum with no characteristic features.

Changes during Drying. Even mild drying of the samples, at room temperature, produces progressive immobilization of most spin probes. The first ones to be immobilized are those whose headgroups are easily attached to silica and whose nitroxide groups are relatively close to the headgroup: CAT 16, 5- and 7-DSA, and doxyl-TMOS (see below). 16-DSA and $C_{12}-NO$ are the last ones to be immobilized. Even after being dried at 80 °C for 2 h, the samples preserve sites with these probes being mobile (Figures 3, left and right). It is notable that under the conditions described the silica frame cross-linking is only

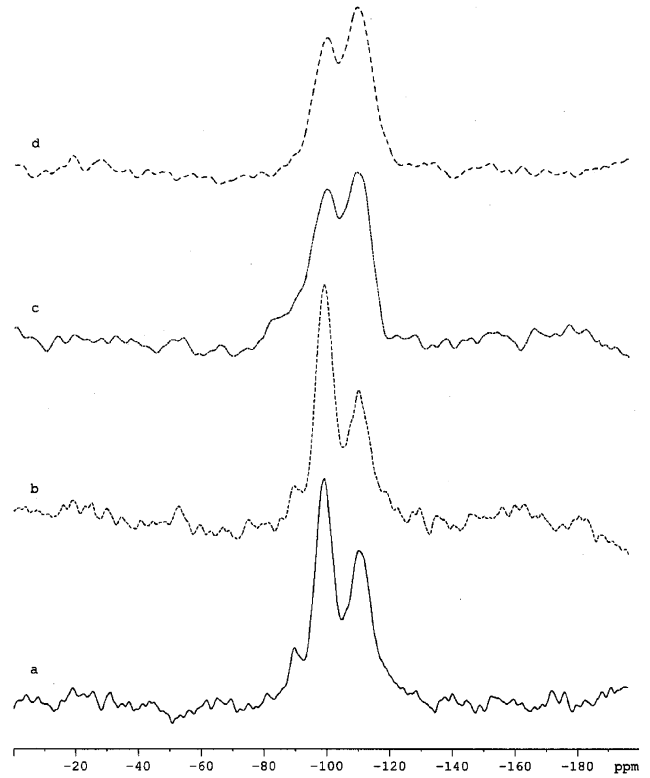

Figure 4. ^{29}Si NMR spectra of the sample $\mathbf{B_o}$: (a) after drying for 2 h at 50 °C, (b) after drying sample a for 2 h at 70 °C, (c) after drying sample b for 2 h at 90 °C, (d) after drying sample c for 2 h at 110 °C. Samples c and d show clearly a decrease in the Q2 signal at − 92 ppm and an increase in the Q4 signal, indicative of increased cross-linking.

incipient.^{29}Si NMR data show (Figure 4) that the connectivity of the silica matrix is very low in the as-synthesized samples: the major peak is Q3 (a Si atom connected to only three other Si atoms), and there is even a small Q2 peak. There is little change in the Q3/Q4 ratio during drying at 50 °C or at 70 °C. This means that at these temperatures the degree of cross-linking is low and the temperature increase brings little change. Thus, changes in the EPR signals are likely to be due to changes in solvation. Only after drying at temperature of 90 °C for 2 h is there a very significant change in the degree of cross-linking (Q2 disappears and Q4 becomes the most intense peak), and the spectrum becomes typical of a rigid framework, quite similar

TABLE 3: Summary of Postsynthesis Adsorption Experiments for the 5-DSA Probe

	pore types		solution		adsorption conditions		type of spectra	
solid/ solution	framework	textural	micelle	emulsion	2 days, stirring	1 day, no stirring	immobilized	"with order"
$\mathbf{B_f/B_0}$	•		•		•		•	
$\mathbf{B_f/B_0}$	•		•			•		
$\mathbf{A_f/B_0}$	•	•	•		•		•	•
$\mathbf{A_f/B_0}$	•	•	•			•		•
$\mathbf{A_f/A_0}$	•	•		•	•		•	•
$\mathbf{A_f/A_0}$	•	•		•		•		•
$\mathbf{A}^a$	•	•		•				•
$\mathbf{B}^a$	•		•				•	

[a] For comparison the results of 5-DSA introduced during precipitation in solids **A** and **B** are also listed.

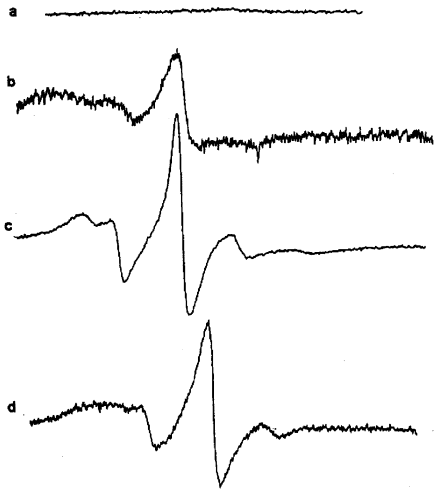

Figure 5. EPR spectra of 5-DSA adsorbed (a) on $\mathbf{B_f}$ from $\mathbf{B_0}$, left 1 day, without stirring; (b) on $\mathbf{B_f}$ from $\mathbf{B_0}$, left 2 days, with stirring; (c) on $\mathbf{A_f}$ from $\mathbf{B_0}$, left 1 day, without stirring; and (d) on $\mathbf{A_f}$ from $\mathbf{B_0}$, left 2 days, with stirring.

Figure 6. EPR spectra of doxyl-TMOS: (a) solution $\mathbf{B_0}$; (b) wet precipitate **B**; (c) precipitate **B** dried at room temperature; (d) same as part b, after total removal of the surfactant, dried at room temperature.

to a spectrum of silica itself. This changes little on further drying at 110 °C and the solid would be expected to be considerably more rigid.

(3) Spin Probes Adsorbed on the Final Silicas $\mathbf{A_f}$ and $\mathbf{B_f}$. Experiments were conducted in which the final solids $\mathbf{A_f}$ and $\mathbf{B_f}$, derived from the corresponding as-synthesized silicas **A** and **B** after surfactant removal, were equilibrated with the starting solutions $\mathbf{A_0}$ and $\mathbf{B_0}$, containing the spin probe 5-DSA. This probe was selected because it presents two qualitatively different types of spectra, when included in samples **A** and **B** during precipitation (see above). Two adsorption procedures have been used: a mild one, leaving the solid in solution, without stirring for 24 h, and a more severe condition, stirring the solution with the solid for 48 h. By these procedures, one or both of the two types of spectra discussed above ("immobilized" and "with order") are observed, depending on circumstances. Table 3 shows the types of spectra obtained for these two adsorption conditions, the aggregate organization in solution and the porosity characteristics of the solids.[9,10] It is clear that the observation of the spectrum "with order" correlates well with the existence of the textural pores, while the immobilized type spectrum, which appears only after adsorption during 2 days with stirring, can be correlated with the framework pores. Thus, for the $\mathbf{B_f/B_0}$ solid/solution system, no spectrum was observed after adsorption under mild conditions (Figure 5a); however, after 2 days with stirring the "immobilized" spectrum of 5-DSA was obtained (as in solid **B**), with weak intensity (Figure 5b). The diffusion of the surfactant into the pores appears to be quite difficult and requires severe conditions, unlike a possible external surface adsorption. Considering also that the solid $\mathbf{B_f}$ has mostly framework pores, the spectrum of the immobilized probe can be assigned to the surfactant aggregates in the framework pores of solid **B**. Adsorption from the same micellar solution $\mathbf{B_0}$ on the solid $\mathbf{A_f}$, which possesses a large proportion of textural pores besides the framework pores, results (under mild conditions) in a high-intensity spectrum "with order" of 5-DSA (Figure 5c), also observed in the sample **A**. This experiment rules out the possibility that the spectrum "with order" would originate from the initial $\mathbf{A_0}$ emulsion, as might have been suspected. Under the more severe adsorption conditions, two overlapped spectra appear (Figure 5d) in this case: one "with order" and one "immobilized" (as in sample $\mathbf{B_f}$, described above). These spectra can be assigned to surfactant aggregates in textural and in framework pores, respectively. The same results have been obtained with the $\mathbf{A_f/A_0}$ system. The much easier access of surfactant and probe to the sites corresponding to the large, textural pores, as compared to the ones in the framework pores, is evident and supports the assignment of the spectrum "with order" to the aggregates in textural pores. These are probably analogue to an adsorbed layer of surfactant on the surface of the textural pores, which can be assimilated with an external surface.

Spin-Labeled TMOS (Doxyl-TMOS). When dissolved in the micellar solution $\mathbf{B_0}$, the doxyl-TMOS probe (10^{-4} M) yields a typical micellar spectrum with three symmetric lines ($a_N = 14.8$ G, $\tau_C = 14.4\ s^{-1}$) (Figure 6a). The spin probe is assumed to be oriented with its hydrophilic part $(MeO)_3Si-$ toward the water/shell interface. After precipitation with TEOS for 18 h by the usual procedure, the probe presented in the filtered moist solid an immobilized type spectrum ($2A_{zz} = 68.8$ G, Figure 6b), similar to that found with 5-DSA in **B**. The same spectrum was

found in the precipitate formed in the first 90 min of reaction. It is an indication that the immobilization of 5-DSA in **B** might be due to interaction with silica precursor elements. Starting with emulsion $\mathbf{A}_0$, where the probe presented also a micellar-type three-line spectrum, the resulted moist solid gave two type of spectra: an immobilized one ($2A_{zz} = 57.1$ G) and a more mobile, micellar-type spectrum. Considering the assignments discussed above for the other spin probes, the immobilized spectrum is consistently assigned to the probe in the small micelles in the framework pores, in strong interaction with the silica interface, while it is tempting to assign the remaining, more mobile spectrum to the surfactant aggregates in the textural pores. As in the case of CAT 16, after total removal of the surfactant from the solid **B** containing the doxyl-TMOS probe (included at the beginning of reaction), the moist solid still showed the spectrum of the probe. After drying, the spectrum of the probe adsorbed on the solid surface (Figure 6d) is significantly different from the one obtained in the presence of the surfactant, a strong indication that in the last case the probe is indeed in the aggregate (Figure 6c).

Conclusions

Our results with spin probes provide information on the structures of surfactant aggregates in the starting solutions $\mathbf{A_0}$ and $\mathbf{B_0}$ and in the precipitates **A** and **B**, as well as after their mild thermal treatment.

In the starting solutions, important differences in the solvation of the aggregates and subsequently in the curvature of their interfaces and in packing of the surfactant have been evidenced, depending on the ethanol/water ratio of the solvent. These proved to have consequences on their interactions with the silica precursor during precipitation and on the type of pores in the final product.

Postsynthesis adsorption experiments with 5-DSA on the solids $\mathbf{A_f}$ and $\mathbf{B_f}$ (after surfactant removal) have enabled us to assign the spectra observed in the precipitates to the two types of pores formed: thus, the "immobilized" spectrum of 5-DSA is observed to appear in framework pores, while observation of the spectrum "with order" is connected with the textural pores. Consequently, the "ordered" type spectrum was assigned to *weakly bound, large aggregates in the textural pore*. By contrast, the immobilized type spectrum of 5-DSA is believed to belong to *small micelles with* a *strong interaction at the interface with the silica framework*. Other results support these assignments. CAT 16 and doxyl-TMOS have only an immobilized type spectrum in **B**, while they have two types of spectra in **A** (an immobilized and a mobile one), corresponding to the two types of aggregates described above, in framework and in textural pores.

Our results also point to the importance of solvation for the surfactant−silica interaction in the case of DDA, a neutral surfactant, and have shown that water and/or ethanol play an important part as intermediates in the weak link of the micelles to the silica, ensuring the partial mobility of the probe polar heads.

These findings, together with the porosity characteristics of the two types of mesoporous silica prepared, have led us to assign the strongly bound micellar aggregates found in the solid precipitated from an ethanol-rich solution, **B**, as being the templates on which mesopores are formed. Their low accessibility (difficult access), as observed with postsynthesis adsorption on $\mathbf{B_f}$, corresponds to the properties of wormhole type pores. In solid **A**, precipitated from a water-rich emulsion, we have evidenced the emulsion type aggregates involved in the formation of the much larger textural pores. The existing framework pores, similar to those in **B**, which could not be evidenced in their presence in the synthesized samples, were clearly observed in post-adsorption experiments.

The existence of small aggregate templates in the synthesis of solid **A**, which is prepared starting from an emulsion, requires the reorganization of the surfactant aggregates during precipitation, i.e., a cooperative process. In the case of solid **B**, starting with a micellar solution with small micelles, close to the size of the resulting mesopores, this does not seem to be necessary.

Acknowledgment. We are grateful to the Royal Society (Great Britain) for a Joint Project Grant and to the Ministry of Education and Research (Romania) for financial support through Grant 842/(1996−2000). D.J.M. thanks the Royal Society for a University Research Fellowship; the authors thank Stewart Tavener for the NMR spectra and Dr. Petre Ionita for preparing the doxyl-TMOS compound.

References and Notes

(1) Beck, J. S.; Vartuli, J. C.; Leonowicz, M. E.; Kresge, C. T.; Scmitt, K. D.; Chu, C. T. W.; Olson, D. W.; Sheppard, E. W.; McCullen, S. B.; Higgins, J. B.; Schlenke, J. L. *J. Am. Chem. Soc.* **1992**, *114*, 10834.
(2) Raimondi, M. E.; Seddon, J. M. *Liq. Cryst.* **1999**, *26*, 305.
(3) Macquarrie, D. J. *Green Chem.* **1995**, *1*, 195.
(4) Macquarrie, D. J. *Chem. Commun.* **1996**, 1961.
(5) Macquarrie, D. J.; Jackson, D. B. *Chem. Commun.* **1997**, 1981.
(6) Macquarrie, D. J.; Mdoe, J. E. G.; Clark, J. H. *Synlett* **1998**, 625.
(7) Macquarrie, D. J.; Jackson, D. B.; Mdoe, J. E. G.; Clark, J. H. *New J. Chem.* **1999**, *23*, 539.
(8) Macquarrie; D. J. Jackson, D. B.; Tailland, S.; Utting, K. A. *J. Mater. Chem.* **2001**, *11*, 1843.
(9) Pauly, T. R.; Liu, Yu; Pinnavaia, T. J.; Billings, S. J.; Ricker, T. P. *J. Am. Chem. Soc.* **1999**, *121*, 8835.
(10) Zhang, W.; Pauly, T. R.; Pinnavaia, T. J. *Chem. Mater.* **1997**, *9*, 2491.
(11) Caldararu, H. *Spectrochim. Acta, Part A* **1998**, *54*, 2309.
(12) Caragheorgheopol, A.; Caldararu, H. *EPR Spin-labeling and Spin Probe Studies of Self-assembled Systems*; Specialist Periodical Reports: Electron Paramagnetic Resonance 17, Royal Society of Chemistry: London, 2000; p 205.
(13) Bakker, M. G.; Turner, G. L.; Treiner, C. *Langmuir* **1999**, *15*, 3078.
(14) Bakker, M. G.; Morris, T. A.; Turner, G. L.; Granger, Ed.; *J. Chromatogr.* **2000**, *743*, 65.
(15) Zhang, J. Y.; Luz, Z.; Goldfarb, D. *J. Phys. Chem. B* **1997**, *101*, 7087.
(16) Zhang, J. Y.; Zimmerman, H.; Luz, Z.; Goldfarb, D. *Stud. Surf. Sci. Catal.* **1998**, *117*, 535.
(17) Galarneau, A.; Di Renzo, F.; Fajula, F.; Mollo, L.; Fubini, B.; Ottaviani, M. F. *J. Colloid Interface Sci.* **1998**, *201*, 105.
(18) Galarneau, A.; Lerner, D.; Ottaviani, M. F.; Di Renzo, F.; Fajula, F.; Fubini, *Stud. Surf. Sci.* **1998**, *117*, 405.
(19) Waggoner, A. S.; Keith, A. D.; Griffith, O. H. *J. Phys. Chem.* **1968**, *72*, 7109.
(20) Knauer, B. R.; Naples, J. J. *J. Am. Chem. Soc.* **1976**, *98*, 4395.
(21) Stone, T. J.; Buckman, T.; Nordio, P. L.; McConell, H. M. *Proc. Natl. Acad. Sci. U.S.A.* **1965**, *54*, 1010.
(22) Seelig, J. *J. Am. Chem. Soc.* **1970**, *92*, 3881; see also Seelig, J. In *Spin Labeling I*; Berliner, L. J., Ed.; Academic Press: New York, San Francisco, CA, and London, 1976; p 373.
(23) Gaffney, B. J. In *Spin Labeling I*; Berliner, L. J., Ed.; Academic Press: New York, San Francisco, CA, and London, 1976; p 567.
(24) Kosower, E. M. *J. Am. Chem. Soc.* **1958**, *80*, 3253.
(25) Caragheorgheopol, A.; R. Bandula, R.; Caldararu, H.; Joela, *J. Mol. Liq.* **1997**, *72*, 105.
(26) Vasilescu, M.; Caragheorgheopol, A.; Caldararu, H.; Bandula, R.; Lemmetyinen, H.; Joela, H. *J. Phys. Chem. B* **1998**, *102*, 7740.
(27) Lasic, D. D.; Hauser, H. *J. Phys. Chem.* **1985**, *89*, 2648.
(28) Haering, G.; Luisi, P. L.; Hauser, H. *J. Phys. Chem.* **1986**, *92*, 3574.